Solid State Communications 147 (2008) 107–110

Contents lists available at ScienceDirect

Solid State Communications

journal homepage: www.elsevier.com/locate/ssc

Magnetic properties of a high energy ball-milled amorphous $Gd_5Si_{1.8}Ge_{1.8}Sn_{0.4}$ alloy

T.B. Zhang [a,b,*], V. Provenzano [b], Y.G. Chen [a], R.D. Shull [b]

[a] School of Materials Science and Engineering, Sichuan University, Chengdu 610065, PR China
[b] Magnetic Materials Group, NIST, 100 Bureau Drive, MS-8552, Gaithersburg, MD 20899, USA

ARTICLE INFO

Article history:
Received 18 March 2008
Received in revised form
30 April 2008
Accepted 2 May 2008 by C. Lacroix
Available online 14 May 2008

PACS:
75.50.Kj
75.30.Sg

Keywords:
A. Amorphous
B. High-energy ball-mill
D. Magnetocaloric effect
D. Magnetic properties

ABSTRACT

Amorphous $Gd_5Si_{1.8}Ge_{1.8}Sn_{0.4}$ has been obtained with the help of a high-energy ball milling technique. XRD and DSC measurements confirm the amorphous nature of the milled alloy. The separation of FC and ZFC curves below the ferromagnetic transition temperature indicates a spin glass-like state in the amorphous alloy. Thermal hysteresis has been significantly reduced in the high energy ball-milled alloy compared with that of a crystalline one. For the amorphous $Gd_5Si_{1.8}Ge_{1.8}Sn_{0.4}$, magnetic phase transition takes place in a wide temperature span and the RC value reaches around 495 J kg^{-1}.

1. Introduction

Considering the high efficiency and environmental friendliness, room temperature magnetic refrigeration has received increasing attention since the discovery of the giant magnetocaloric effect in $Gd_5Si_2Ge_2$ [1]. Much research has been carried out to explore new magnetic refrigerant materials for use at or near room temperature. The first order magnetic-crystallographic transition (FOMT) near T_C in $Gd_5(Si_xGe_{1-x})_4$ ($x \sim 0.5$) has now been well accepted as the mechanism for the giant magnetocaloric effect. Up to now, the $Gd_5(Si_xGe_{1-x})_4$ intermetallic compounds look more suitable for near room temperature applications considering the MCE properties, the resistance to corrosion in air and water comparing with other magnetic refrigerants such as $La(Fe_xSi_{1-x})_{13}$, $MnFe(P_{1-x}As_x)$, $MnAs_{1-x}Sb$, Ni_2MnGa et al. [2]. But the high price of Gd and Ge is the main obstacle for practical use of $Gd_5(Si_xGe_{1-x})_4$ as magnetic refrigerants. In addition, the required high temperature heat treatment for the giant MCE in this series of alloys also increases the manufacturing cost. More recent research has shown that the monoclinic phase accounting for the room temperature magnetocaloric effect in $Gd_5Si_2Ge_2$ is easy to form with the addition of Sn. Sn-doped alloys exhibit significant MCE at near room temperature due to the nearly single $Gd_5Si_2Ge_2$-type phase in the as-cast state [3]. A suitable Sn substitution for Ge and Si could decrease the cost of the raw materials in Gd-based refrigerant alloys to some extent.

In Sn-doped alloys, large thermal and magnetic hystereses are both observed in addition to the giant magnetocaloric effect as the $Gd_5(Si_xGe_{1-x})_4$ ($x \sim 0.5$) alloys [4–6]. Because of the coincidence of hysteresis with the giant magnetocaloric effect, it is believed that the first order magnetic-crystallographic transformation (FOMT) also accounts for hysteresis phenomena. For practical applications, hysteresis has to be considered due to the energy loss in the refrigeration circle. Experimental research has shown transition elements (Mn, Fe, Co, Ni) and some other small metal additions could decrease the hysteresis of $Gd_5Si_2Ge_2$ remarkably through the formation of the second phase [5,7,8]. The suppression of FOMT near T_C in $Gd_5Si_2Ge_2$ results in a hysteresis reduction with the addition of transition elements. According to the recent results, magnetic and thermal hystereses of $Gd_5Si_{1.8}Ge_{1.8}Sn_{0.4}$ with FOMT could also be significantly reduced without changing the monoclinic structure in the as-cast state with the help of the melt-spun technique [6]. The crystalline grain size of spun ribbons is much smaller than that of the as-cast alloy and the dimension of

* Corresponding address: School of Materials Science and Engineering, Sichuan University, No. 24, South Settion, 1st Ring Road, Chengdu 610065, PR China. Tel.: +86 28 85405670; fax: +86 28 85407335.
E-mail address: scuztb@sohu.com (T.B. Zhang).

0038-1098/$ – see front matter © 2008 Elsevier Ltd. All rights reserved.
doi:10.1016/j.ssc.2008.05.009

the magnetic domain is probably the same. The hysteresis loss reduction in melt spun $Gd_5Si_{1.8}Ge_{1.8}Sn_{0.4}$ could be understood as follow: Firstly, separation of the ferromagnetic transition and crystal structure transformation suppresses the FOMT in the as-cast state; In addition, the decrease in dimensions of magnetic domains and crystalline grain size favors domains to be easily turned and correspondingly reduces hysteresis loss.

In the present work, we investigate the magnetocaloric effect and related magnetic properties of high-energy ball milled $Gd_5Si_{1.8}Ge_{1.8}Sn_{0.4}$. Powder X-ray diffraction and DSC measurements indicate the amorphous nature of the milled $Gd_5Si_{1.8}Ge_{1.8}Sn_{0.4}$ alloy. We present another efficient way to reduce the hysteresis of $Gd_5Si_{1.8}Ge_{1.8}Sn_{0.4}$ with FOMT and try to explore new magnetic refrigerants with a large RC value and small hysteresis loss.

2. Experimental details

The master $Gd_5Si_{1.8}Ge_{1.8}Sn_{0.4}$ alloy was prepared by the arc-melt method in a copper crucible using 99.94 wt% Gd and high purity Si and Ge (both >99.99 wt%) under the protection of an argon atmosphere. During melting, the sample was homogenized by turning the buttons over and re-melting five times to ensure homogeneity. Consequently, the alloy was ball milled in a SPEX8000 type high-energy shaker mill machine. All sample handling was performed under argon in a glove box to prevent oxygenation of the alloy in the milling process. Particles were placed into a steel vial along with 12 mm diameter hardened steel balls. The vial was then sealed in an argon-filled glove box. The ball to powder ratio used was 10:1 by weight. Nine stainless-steel balls (2×12.56 mm and 7×6.32 mm in diameter) were used in the milling process. Amorphous $Gd_5Si_{1.8}Ge_{1.8}Sn_{0.4}$ particles were prepared by high energy ball milling for 1 h.

The ball-milled $Gd_5Si_{1.8}Ge_{1.8}Sn_{0.4}$ alloy was first examined with the help of powder XRD. X-ray diffraction data were collected at room temperature on the D/max 2500 diffractometer using Cu K_α radiation between 20° and 60° (2θ). The voltage and anode current were 40 kV and 250 mA, respectively. The temperature dependence of magnetization (M–T) was performed on a quantum designed MPMS-7 type SQUID magnetometer. Prior to the measurement, the sample was cooled in a zero-field from room temperature to 5 K in the absence of a magnetic field. Then temperature dependent magnetization from 4.2 to 350 K for an applied field of 0.1 T in the warming process was first recorded and denoted as ZFC. After that, thermomagnetic curves were measured in 0.1 T during cooling (FC) and heating (FH) without removing the external field to investigate thermal hysteresis of the sample. The magnetization isotherms (M–H) from 10 to 300 K were collected on the same magnetometer in a field up to 3980 kA m^{-1} (5 T) with a temperature interval of 10 K for the calculation of magnetic entropy change. Thermal analysis of the milled alloy was used to determine the glass transition and the crystallization behavior; the measurement was carried out by a Netzsch differential scanning calorimeter (DSC) using a heating rate of 5 K/min under the protection of a high purity argon atmosphere.

3. Results and discussion

Fig. 1 shows the X-ray diffraction pattern of the ball-milled $Gd_5Si_{1.8}Ge_{1.8}Sn_{0.4}$ alloy. Bragg peaks in the XRD pattern of the crystalline alloy [6] are all suppressed in the high energy ball-milled sample. Only two scattered broad diffraction peaks around 32° and 53° (2θ) are observed in Fig. 1 indicating the amorphous nature of the high-energy ball milled $Gd_5Si_{1.8}Ge_{1.8}Sn_{0.4}$. In the experimental milling process, the crystalline state is destroyed by the high energy introduced to the alloy. Milling-induced phase

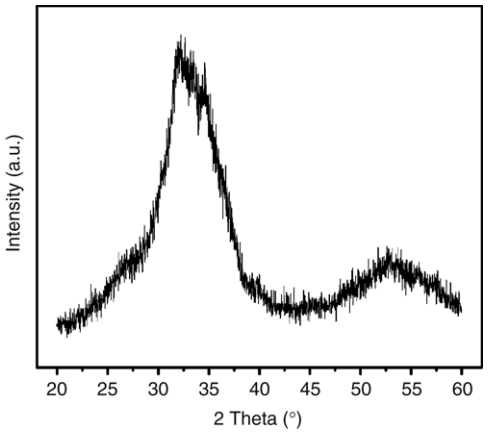

Fig. 1. Powder X-ray pattern of high-energy ball milled $Gd_5Si_{1.8}Ge_{1.8}Sn_{0.4}$ alloy.

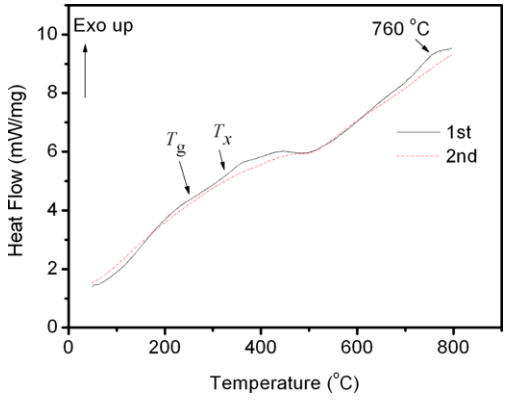

Fig. 2. DSC curve for high-energy ball milled $Gd_5Si_{1.8}Ge_{1.8}Sn_{0.4}$ alloy at a constant heating rate of 5 K/min.

transition from monoclinic crystal structure to the disordered amorphous state has taken place in $Gd_5Si_{1.8}Ge_{1.8}Sn_{0.4}$. Due to the exchange interaction's and crystalline electric field's fluctuation originating from structural disorder, the amorphous materials always broadens the magnetic transition from paramagnetic to a magnetically ordered state [9]. The broadness of the magnetic transition temperature span always means a possible increase of refrigerant capacity. Therefore, a large RC value and small hysteresis loss are expected to be obtained in amorphous $Gd_5Si_{1.8}Ge_{1.8}Sn_{0.4}$.

To further confirm the XRD result, the DSC curve is shown in Fig. 2. In order to clearly investigate the crystalline behavior of the milled amorphous alloy, we re-collected the DSC trace as the sample had been slowly cooled down to room temperature in the first measurement. From Fig. 2, it is clear that a broad scatter peak from ∼150 to ∼450 °C still exists in the "annealed" amorphous $Gd_5Si_{1.8}Ge_{1.8}Sn_{0.4}$ alloy. The heat flow in the second measurement around 300 °C indicates the reversible phase transformation's signal contribution to the first trace in addition to crystallization of the amorphous state. According to the DSC curve in Fig. 2, the glass transition temperature (T_g) and crystallization temperature (T_x) of amorphous $Gd_5Si_{1.8}Ge_{1.8}Sn_{0.4}$ alloy are determined as ∼260 and ∼330 °C, respectively. In addition, there is another phase transition around 760 °C in the amorphous alloy. The disappearance of the high temperature endothermic peak in the second trace indicates that this phase transformation is irreversible.

Fig. 3 displays the ZFC, FC and FH thermomagnetic curves (M–T) for milled $Gd_5Si_{1.8}Ge_{1.8}Sn_{0.4}$ amorphous alloy. In the ZFC curve, magnetization keeps low values and a small positive slope with increase in temperature. A cusp with a maximum around 30 K

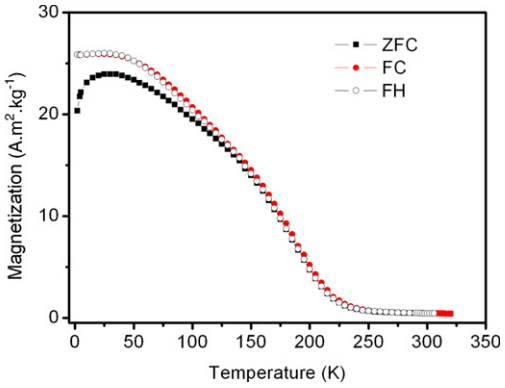

Fig. 3. ZFC, FC, and FH thermomagnetic curves for milled $Gd_5Si_{1.8}Ge_{1.8}Sn_{0.4}$ alloy in the field of 0.1 T.

in the ZFC curve indicates the possible T_f of a spin glass in the experimental sample. During the field cooled process (FC), the milled amorphous alloy firstly transforms from paramagnetism to a mixed magnetic state (i.e.: superparamagnetism and antiferromagnetic), and then to ferromagnetic in a relative large temperature span (from ~240 K to ~30 K). The FC and FH curves are almost identical and thermal hysteresis, estimated from the minimum of dM/dT between heating and cooling in the transition region, could be neglected. The FOMT observed in crystalline $Gd_5Si_{1.8}Ge_{1.8}Sn_{0.4}$ has been suppressed in the high energy ball milled amorphous magnetic particles. The small dimensions of the magnetic domains makes the moments easily paralleled with the external field. As has been observed in other Gd-based compounds [10,11], the separation of FC and ZFC curves below the ferromagnetic transition temperature is expected to be associated with the spin glass-like state coexisting with ferromagnetism in amorphous $Gd_5Si_{1.8}Ge_{1.8}Sn_{0.4}$ alloy. The ferromagnetism of the as-cast state at low temperatures has been partially destroyed due to the high energy transmitted to the alloy in the milling process.

Magnetization isotherms (M–H) for high energy ball milled $Gd_5Si_{1.8}Ge_{1.8}Sn_{0.4}$ at various temperatures with a field up to 5 T are displayed in Fig. 4(a). The amorphous alloy shows typical paramagnetic behavior at temperatures above 180 K. At temperatures between 60 and 170 K, the alloy shows superparamagnetic characteristic as shown by the appearance of curvature in the M–H plots. Magnetization isotherms near T_C indicate that there is no field-induced structure transition as the magnetic transition takes place in the amorphous alloy. Below ~60 K, magnetization rises sharply at the low field and increases gradually until saturation with a further increase of the external field indicating the existence of a ferromagnetic state. The ordered magnetic moment for the $Gd_5Si_{1.8}Ge_{1.8}Sn_{0.4}$ alloy, extrapolated to zero magnetic field, is 7.62 μ_B/Gd, while for elemental Gd is 7.0 and 7.63 μ_B from theory and experiment, respectively [12,13]. The saturated magnetic moment shows that the as-cast $Gd_5Si_{1.8}Ge_{1.8}Sn_{0.4}$ has a nearly completely collinear spin structure. In the amorphous state, the effective magnetic moment is about 5.66 μ_B/Gd calculated by extrapolating the M–H to the infinite field. The much smaller magnetic moment in the milled alloy suggesting the collinear spin structure in crystalline alloy has been changed to a non-collinear one. As a result, the Gd–Gd super-exchange between the inter Gd_5T_4 (T: Si, Ge, Sn) slab must be weakened or even suppressed in the amorphous state and the magnetic transition temperature decreases correspondingly comparing with that of the as-cast alloy [13,14]. For this reason, the ferromagnetic transition of the as-cast alloy splits for the appearance of the super-paramagnetic or possible anti-ferromagnetic state. Moreover, the magnetic transition takes place in a large temperature span at a relative low temperature for the milled amorphous $Gd_5Si_{1.8}Ge_{1.8}Sn_{0.4}$ alloy.

On the basis of the magnetization isotherms (M–H) at different temperatures, the $-\Delta S_{Mag}$ (T) curve for amorphous $Gd_5Si_{1.8}Ge_{1.8}Sn_{0.4}$ constructed using Maxwell equation is shown in Fig. 4(b). The amorphous alloy shows a moderate magnetocaloric effect and the maximal magnetic entropy change is ~4.3 J kg^{-1} K^{-1}. As expected, the half width of $-\Delta S_{Mag}$ peak is considerably broader than that of the as-cast alloy. From the thermomagnetic curves in Fig. 3, it can be seen FC and ZFC curves separate around the temperature where the maximal magnetic entropy change appears in Fig. 4. This coincidence indicating the spin glass state formation during the magnetic transition plays an important role for the magnetocaloric effect of the amorphous $Gd_5Si_{1.8}Ge_{1.8}Sn_{0.4}$ alloy. In addition, the superparamagnetism or AFM to FM transformation in the same temperature region also partially contributes to the magnetic entropy change. With temperatures at half-maximum of the $-\Delta S_{Mag}$ peak as the integration limit, the RC value calculated by numerically integrating the area under the $-\Delta S_{Mag}$ versus T curve using the method in Ref. [15] is around 495 J kg^{-1}, which increases ~35% comparing with that of the as-cast alloy (366 J kg^{-1}).

4. Conclusions

In summary, the magnetocaloric effect, hysteresis and crystalline behavior of high-energy ball milled amorphous $Gd_5Si_{1.8}Ge_{1.8}Sn_{0.4}$ have been investigated. X-ray diffraction and thermal analysis confirm the amorphous nature of the milled alloy. The ferromagnetic transition temperature of amorphous $Gd_5Si_{1.8}Ge_{1.8}Sn_{0.4}$ anticipating from the thermomagnetic curves is lower than that of the as-cast state and no thermal hysteresis is

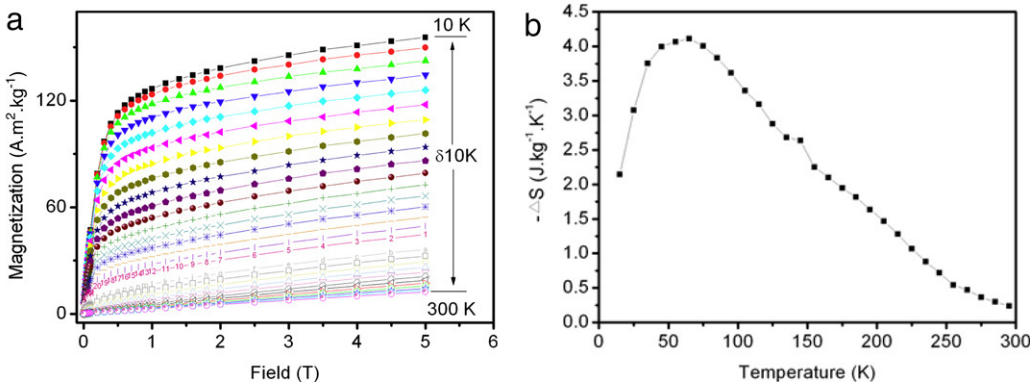

Fig. 4. (a) Magnetization isotherms and (b) magnetic entropy change ($-\Delta S_{Mag}$) of high-energy ball milled $Gd_5Si_{1.8}Ge_{1.8}Sn_{0.4}$ for a 0–50 kOe field change.

observed in the milled alloy. Magnetic measurements show the reduction of hysteresis, broadening of the magnetic transition temperature span and an increase of the total refrigerant capacity in the ball-milled amorphous $Gd_5Si_{1.8}Ge_{1.8}Sn_{0.4}$ alloy.

Acknowledgements

This work is supported by the National High Technology Research and Development Program (2007AA03Z440) and the Key Project of National Natural Science Foundation (50731007) of PR China. T.B. Zhang also acknowledges the financial support from the China Scholarship Council (2007U24056). Dr. KW Moon from NIST is gratefully appreciated for his help in DSC measurement.

References

[1] V.K. Pecharsky, K.A. Gschneidner Jr., Phys. Rev. Lett. 78 (1997) 4494.
[2] K.A. Gschneidner Jr., V.K. Pecharsky, A.O. Tsokol, Rep. Prog. Phys. 68 (2005) 1479.
[3] T.B. Zhang, Y.G. Chen, Y.B. Tang, T. Ren, M.J. Tu, Mater. Charact., in press (doi:10.1016/j.matchar.2007.12.004).
[4] L. Morellon, J. Blasco, P.A. Algarabel, M.R. Ibarra, Phys. Rev. B 62 (2000) 1022.
[5] V. Provenzano, A.J. Shapiro, R.D. Shull, Nature 429 (2004) 853.
[6] T.B. Zhang, Y.G. Chen, Y.B. Tang, J. Phys. D: Appl. Phys. 40 (2007) 5778.
[7] T.B. Zhang, Y.G. Chen, Y.B. Tang, H.J. Du, T. Ren, M.J. Tu, J. Alloy. Comp. 433 (2007) 18.
[8] R.D. Shull, V. Provenzano, A.J. Shapiro, A. Fu, M.W. Lufaso, J. Karapetrova, G. Kletetschka, V. Mikula, J. Appl. Phys. 99 (2006) 08K908.
[9] A.M. Tishin, Y.I. Spichkin, The Magnetocaloric Effect and its Applications, Institute of Physics Publishing, Bristol, 2003.
[10] S.B. Roy, M.K. Chattopadhyay, P. Chaddah, J.D. Moore, G.K. Perkins, L.F. Cohen, K.A. Gschneidner Jr., V.K. Pecharsky, Phys. Rev. B 74 (2006) 012403.
[11] R.D. McMichael, J.J. Ritter, R.D. Shull, J. Appl. Phys. 73 (1993) 6946.
[12] E.M. Levin, V.K. Pecharsky, K.A. Gschneidner Jr., P. Tomlinson, J. Magn. Magn. Mater. 210 (2000) 181.
[13] E.M. Levin, V.K. Pecharsky, K.A. Gschneidner Jr., Phys. Rev. B 62 (2000) R14625.
[14] D. Haskel, Y.B. Lee, B.N. Harmon, Z. Islam, J.C. Lang, G. Srajer, Y. Mudryk, J.K.A. Gschneidner, V.K. Pecharsky, Phys. Rev. Lett. 98 (2007) 247205.
[15] K.A. Gschneidner Jr., V.K. Pecharsky, A.O. Pecharsky, C.B. Zimm, Mater. Sci. Forum 315-317 (1999) 69.